Six-dimensional quantum treatment of the vibrations of diatomic adsorbates on solid surfaces: CO on Cu(100)

Atul Bahel and Zlatko Bačić

Citation: The Journal of Chemical Physics **111**, 11164 (1999); doi: 10.1063/1.480494
View online: http://dx.doi.org/10.1063/1.480494
View Table of Contents: http://scitation.aip.org/content/aip/journal/jcp/111/24?ver=pdfcov
Published by the AIP Publishing

Six-dimensional quantum treatment of the vibrations of diatomic adsorbates on solid surfaces: CO on Cu(100)

Atul Bahel[a] and Zlatko Bačić[b]
Department of Chemistry, New York University, 100 Washington Square East, New York, New York 10003

(Received 22 July 1999; accepted 29 September 1999)

Computational methodology for exact quantum 6D calculations of the vibrational eigenstates, energy levels, and wave functions of a diatomic molecule adsorbed on a rigid corrugated surface is presented. It is intended for adsorbates executing coupled, strongly anharmonic large-amplitude vibrations. Surface nonrigidity is introduced in an approximate way, by means of a simplified surface-mass model. Using this methodology, we calculate the vibrational levels of CO/Cu(100) for all four isotopomers of CO, $^{12}C^{16}O$, $^{13}C^{16}O$, $^{12}C^{18}O$, and $^{13}C^{18}O$. The empirical potential by Tully and co-workers [J. C. Tully, M. Gomez, and M. Head-Gordon, J. Vac. Sci. Technol. A **11**, 1914 (1993)] is employed. Our calculated fundamental frequencies of CO/Cu(100) vibrations are compared to those from earlier theoretical treatments on the same potential, as well as with the experimental frequencies and isotope frequency shifts. In addition to 6D calculations, we perform 5D (rigid CO) and 4D (fixed-site) quantum calculations, which provide information about the couplings among the vibrational modes of CO on Cu(100). Excited levels of the lowest-frequency in-plane (doubly degenerate) frustrated translation mode are analyzed and assigned. © *1999 American Institute of Physics.* [S0021-9606(99)71248-1]

I. INTRODUCTION

Quantitative description of adsorbate–substrate interactions is an essential prerequisite for accurate quantum and classical simulations of fundamental processes at surfaces, such as adsorption and desorption, surface diffusion, and chemical reactivity. One of the most direct probes of the interaction potentials between adsorbates and solid surfaces is the spectroscopy of the vibrations of the adsorbed molecules. Adsorption of a molecule to a surface gives rise to six vibrational modes (five for linear molecules) with rather low frequencies, which correspond to the bound motions of the whole molecule relative to the surface. These ''external'' modes correlate with the translational and rotational degrees of freedom of the free molecule, which become ''frustrated'' upon adsorption. For this reason, they are referred to as the frustrated translation and rotation modes. Interaction with the surface also affects the high-frequency intramolecular, or ''internal'' vibrational modes localized within the molecule, shifting their frequencies away from the gas-phase values.

Extracting the information about the adsorbate–substrate potential energy surface (PES) which is contained in the vibrational spectra of the adsorbed molecule is a formidable task. Broadly speaking, it involves two steps. The first step is construction of the PES, (semi)empirically or on the basis of *ab initio* calculations. In the second step, vibrational excitation energies and other observables are calculated for this multidimensional PES and compared to experimental data. Only through such direct comparison between theory and experiment can one assess the quality of the PES and systematically refine it by fitting to the spectroscopic data. Obviously, the feasibility of this procedure depends critically on the ability to perform quantum dynamical calculations accurately and efficiently.

A rigorous calculation of the vibrational spectrum of an adsorbed molecule in principle requires a high-level treatment of:

(i) Fully coupled anharmonic external and internal vibrational modes of the adsorbate.
(ii) Phonons of the solid substrate in the frequency range of the external adsorbate vibrations, which can potentially mix with the latter.
(iii) Coupling of the vibrations of the adsorbed molecule to the substrate phonons and, possibly, to electronic states of the solid.

A comprehensive quantum treatment which would encompass (i)–(iii) has not been carried out to data for any realistic system, and is likely to remain prohibitively difficult in the foreseeable future. Most theoretical approaches to this problem have generally addressed (i) with varying levels of rigor, either leaving out (ii) and (iii) or treating them more approximately. A notable attempt to treat (i)–(iii), albeit within a harmonic force-constant model, was made recently by Lewis and Rappe,[1,2] who investigated the vibrational properties of a CO adlayer on Cu(100). They modeled the copper substrate by a multilayer slab sufficiently large to accomodate the long-wavelength bulk phonons. Their studies for the first time treated on equal footing all atoms of both the adsorbate and the substrate. But, owing to the very high dimensionality of the CO/Cu(100) model system considered, vibrational calculations were tractable only in the harmonic

[a]Present address: Department of Chemistry and Biochemistry, University of Notre Dame. Notre Dame. Indiana 46556.
[b]Author to whom correspondence should be addressed. Electronic mail: zlatko.bacic@nyu.edu

normal-mode approximation. While the harmonic treatment yielded valuable insight into the mechanism of rapid vibrational relaxation observed for CO on Cu(100),[3,4] calculation of the frequencies of external and internal vibrational modes of adsorbed CO (and molecular adsorbates in general) sufficiently accurate for unambiguous evaluation of the PES employed (by comparison to experiment) needs to go beyond the harmonic model and include anharmonic mode coupling.

This important step was taken in the vibrational self-consistent field (VSCF) calculations of CO/Cu(100) by Bowman and co-workers.[5,6] In the VSCF approach to a multimode problem,[7,8] the total vibrational wave function is approximated by a simple product of the variationally best single-mode wave functions, which are determined self-consistently. The vibrational Hamiltonian is commonly expressed in the normal-mode coordinates, but the anharmonicity of the PES is retained, i.e., the harmonic approximation is not made. The SCF modes are coupled approximately, in a mean-field fashion; each mode moves in a one-dimensional effective potential obtained by averaging the PES over all other vibrations. However, since the VSCF calculations are much more computationally demanding than the harmonic treatment, it was not possible to include the vibrations of a substantial number of substrate (copper) atoms. The 6D VSCF calculations of CO/Cu(100) considered the six CO–Cu normal modes arising from the motions of the CO molecule alone (with negligible contribution from the Cu-atom motion).[5] The subsequent 9D VSCF calculations[6] were extended to include also the three normal modes of the single Cu atom bound to CO.

In this article, we describe a computational methodology for exact quantum 6D calculations of the vibrational energy levels of a diatomic molecule adsorbed on a rigid corrugated surface. Unlike the VSCF approach above, our method treats the couplings between the six vibrational degrees of freedom of the diatomic adsorbate without any approximation, yielding ground and excited vibrational eigenstates which are numerically exact for the 6D PES employed. The quantum 6D methodology presented here is particularly well suited for calculating accurately the energy levels and wave functions of adsorbed diatomic molecules which exhibit strongly coupled, anharmonic large-amplitude vibrations. The molecule can be adsorbed at surface steps or defects, or on arbitrarily shaped clusters. The surface-atom motion is introduced in the spirit of the surface-mass model of Luntz and Harris,[9] by defining the reduced mass of the diatom relative to the surface so as to include the mass of the surface atom to which the molecule is bound.

We apply this 6D treatment to the vibrations of CO/Cu(100), a prototype adsorbate–substrate system whose vibrational dynamics has been intensely studied in recent years. The fundamental frequencies have been measured for its six molecular vibrational modes,[10–12] the C–O stretch (ν_1), 2079 cm^{-1}, the CO–Cu stretch (ν_2), 345 cm^{-1}, the doubly degenerate frustrated rotation (ν_3), 287 cm^{-1}, and the doubly degenerate frustrated translation (ν_4), 32 cm^{-1}. The vibrations of CO on Cu(100) have been investigated theoretically in the above mentioned studies by Lewis and Rappe,[1,2] Bowman *et al.*,[5,6] and others. The quantum 6D calculations reported in this work were performed for all four isotopomers of CO, $^{12}C^{16}O$, $^{13}C^{16}O$, $^{12}C^{18}O$, and $^{13}C^{18}O$, on the empirical PES for CO/Cu(100) developed by Tully and co-workers.[13,14] They used it in stochastic molecular dynamics simulations of vibrational relaxation of the adsorbed CO molecule. Our 6D results for $^{12}C^{16}O$ are compared to those from the VSCF calculations of CO/Cu(100).[5,6] carried out on the same PES. In addition, direct comparison is made with the measured frequencies of the five external vibrational modes of CO on Cu(100), which are available for the four CO isotopomers,[11] allowing a rather strict test of the PES. The quantum 6D calculations in the present work provide a comprehensive description of the molecular vibrations of the adsorbed CO molecule. In particular, we analyze the level structure and assignments of the excited (doubly degenerate) frustrated translation mode ν_4 parallel to the surface. As the lowest-frequency external mode of CO/Cu(100), it is thermally excited in virtually all experimental situations and is thought to provide a conduit for vibrational energy transfer between the CO adsorbate and the copper substrate.[3,4,15] Comparison with lower-dimensional 5D (rigid CO) and 4D (fixed-site) quantum calculations gives information about the coupling between different vibrational modes of CO on Cu(100) and their effects on the energy levels.

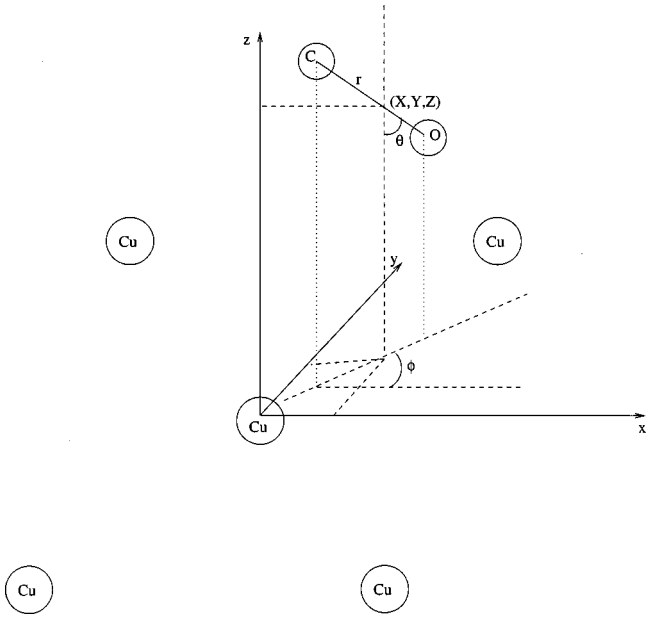

FIG. 1. The coordinate system used in the present work.

In Sec. II we describe the 6D bound state methodology for adsorbate vibrations. Section III deals with the computational aspects of this work. The results of the calculations are presented and discussed in Sec. IV. A summary and conclusions are given in Sec. V.

II. THEORY

A. Six-dimensional Hamiltonian

1. Rigid-surface model

Vibrations of a diatomic molecule on a rigid (static) corrugated surface can be described fully by the set of six coordinates (x,y,z,r,θ,ϕ) shown in Fig. 1; x, y, and z are the

three Cartesian coordinates of the molecule's center of mass, r is the distance between the two atoms in the molecule, and θ and ϕ are the polar angles specifying the orientation of the molecular axis relative to the surface. The 6D vibrational Hamiltonian in terms of these coordinates is

$$H^{6D}=-\frac{\hbar^2}{2\mu}\left(\frac{\partial^2}{\partial x^2}+\frac{\partial^2}{\partial y^2}+\frac{\partial^2}{\partial z^2}\right)-\frac{\hbar^2}{2\mu_d}\frac{\partial^2}{\partial r^2}+\frac{\mathbf{j}^2}{2\mu_d r^2}+V(x,y,z,r,\theta,\phi). \quad (1)$$

In Eq. (1), μ is the reduced mass of the diatomic molecule relative to the metal surface. It is defined as $M_dM_s/(M_d+M_s)$, where M_d is the mass of the diatomic molecule and M_s is the mass of the surface atom(s) to which the molecule is bound. For a static surface $M_s=\infty$, and therefore μ is equal to the mass M_d of the diatomic molecule. Also appearing in Eq. (1) are μ_d and $\mathbf{j}$, the reduced mass and the angular momentum operator, respectively, of the diatomic molecule, while V is the 6D molecule–surface interaction potential. The Hamiltonian in Eq. (1) includes all six molecular degrees of freedom of the adsorbate–substrate system, five of which are the external modes corresponding to frustrated translations and rotations of the whole adsorbed molecule and one is the intramolecular vibration of the diatomic molecule. It allows a rigorous, fully coupled quantum mechanical description of the vibrational dynamics of a diatomic adsorbate on a static surface. The same Hamiltonian (minus the diatomic stretching vibration term) was used by us to calculate the intermolecular vibrational eigenstates of HF in Ar_nHF clusters,[16–18] and also in the recent 6D quantum dynamical investigations of the dissociative adsorption of H_2 on Cu(100).[19–21]

Six-dimensional vibrational eigenstates of the above Hamiltonian are calculated using the computational scheme outlined in Sec II B.

2. Surface-mass model

The rigid surface assumption above is most accurate for systems where a light molecule like H_2 is bound to heavy surface atom(s). In such cases, characterized by the small M_d/M_s ratio, the coupling of the vibrations of the adsorbed molecule to the motions of the surface atoms is expected to be the weakest. When the adsorbed molecule is heavier, such as CO, the coupling to the substrate vibrations increases and treating the surface as rigid is likely to introduce significant errors in the calculated adsorbate vibrational frequencies. This is evident already from the comparison of the values which μ in Eq. (1) has for rigid and nonrigid surfaces, taking CO/Cu(100) as an example. In the rigid surface (RS) treatment where $M_s=\infty$, $\mu=M_{CO}=28.01$ amu; for a nonrigid surface where $\mu=M_{CO}M_s/(M_{CO}+M_s)$. and taking $M_s=63.55$ amu, the mass of a single Cu atom which vibrates together with the CO molecule bound to it (which, as discussed below, is a reasonable assumption), μ is equal to 19.44 amu. This is 30.6% smaller than the RS value. For comparison, in the case of the H_2 molecule on a Cu surface, the μ values for the rigid and nonrigid surface (making the same assumptions about M_s as above), 2 and 1.94 amu, respectively, differ by only 3%.

Since $1/\mu$ multiplies the kinetic energy operator for the Cartesian coordinates x, y, and z in Eq. (1), it is clear that using the RS and nonrigid surface values for μ will result in significantly different CO/Cu(100) vibrational frequencies, especially those of the in-plane and out-of-plane CO vibrations which are associated (mainly) with this term in the Hamiltonian. This is borne out by our calculations discussed in Sec. IV. Moreover, these results show that the ordering of the vibrational fundamentals measured for CO/Cu(100) can be reproduced *only* when the *nonrigid* surface value of μ is employed in the calculations.

Replacing $\mu=M_d$ with $\mu=M_dM_s/(M_d+M_s)$ in Eq. (1) is the simplest, albeit approximate, way of introducing the surface-atom motions in the treatment the vibrations of the adsorbed molecule, without increasing either its dimensionality or complexity. It implicitly involves the following approximations: (i) the adsorbate's center-of-mass motion is coupled to the motion of a single surface atom with mass M_s; (ii) the surface atom is taken to move freely, which physically implies that (a) the surface-atom motions have large amplitude and low frequency, and (b) the details of the interaction between surface atoms can be ignored; (iii) the surface-atom motion does not modify the interaction potential between the adsorbed molecule and the (static) surface.

The above ansatz is closely related to the surface-mass model of Luntz and Harris,[9] which was developed to explain the strong surface-temperature dependence observed for the dissociation of CH_4 on metal surfaces. The same model was later used to allow for nonrigidity of the substrate in the quantum-mechanical calculations of rates for various gas-surface processes.[22] In addition to the approximations (i)–(iii) above, the surface-mass model also assumes that the surface-mass M_s moves with a velocity sampled from a Boltzmann distribution for a given surface temperature.[9,22] Although this feature is not utilized in our calculations, the Hamiltonian in Eq. (1) with $\mu=M_dM_s/(M_d+M_s)$ will be referred to as the surface-mass (SM) model.

The SM model assumes that the vibrations of the adsorbed molecule couple strongly to a very small portion of the substrate, typically one surface atom, directly beneath the adsorbate. The same assumption underlies most other microscopic theoretical studies, such as the VSCF calculations of CO/Cu(100) by Bowman and co-workers.[5,6] Their 9D VSCF calculations include the three normal modes of the Cu atom bound to CO. These highly localized treatments of substrate nonrigidity may not capture all aspects of the coupled adsorbate–substrate vibrational dynamics. For instance, in their normal-mode treatment of the vibrations of a CO adlayer on Cu(100), Lewis and Rappe[1,2] found that the frustrated translation motion of the CO molecule was strongly mixed with the long-wavelength bulk copper phonons at the same frequency. This resulted in a decay time of 3.0 ps for the frustrated translation mode, which agrees very well with the experimental result, 2.3 ± 0.4 ps.[3,4] The fundamental frequencies which these calculations yielded are discussed in Sec. IV C.

B. 6D bound state methodology

The computational methodology used to calculate the energy levels and wave functions of the 6D Hamiltonian in Eq. (1) is an extension of that developed by us for the 5D intermolecular vibrational eigenstates of Ar_nHF van der Waals (vdW) clusters.[16–18] This 5D bound state method was designed for efficient and accurate calculation of the vdW vibrational levels of a broad class of floppy systems where a diatomic molecule (its bond length fixed) is bound to a much heavier, arbitrarily shaped entity (which could be a large molecule, a cluster, a fragment of a cryogenic matrix, or a portion of a solid surface), treated as internally rigid. In the present work, this methodology is extended to 6D, by coupling explicitly the vibration of the diatomic adsorbate to the five external degrees of freedom considered previously.

At the heart of our 6D (and earlier 5D[16–18]) bound state methodology is the sequential diagonalization and truncation method of Bačić and Light,[23–26] capable of reducing drastically the size of the final Hamiltonian matrix, which otherwise becomes prohibitively large for realistic 5D and 6D problems. In this approach, the full-dimensional Hamiltonian matrix is partitioned approximately into a hierarchy of intermediate Hamiltonians of increasing dimensionality. In a procedure which can be repeated several times, sets of eigenvectors of lower-dimensional Hamiltonians, sharply truncated by an energy cutoff criterion, serve as the basis for the Hamiltonians in the next higher dimension. Each cycle of the sequential diagonalization and truncation typically reduces the basis set size by a factor of 3–5, without any loss of accuracy.[18,23–28] This is possible because the intermediate eigenvector bases, being the solutions of coupled multimode problems of lower dimensions, already contain a significant part of the full solution.

The 5D bound state methodology, in which the diatomic bond length is held fixed, is discussed extensively in Ref. 18. Therefore, only the inclusion of the vibration of the diatomic molecule in the 6D treatment is described here; whenever possible, we adhere to the notation used in Ref. 18. The initial 6D basis, which is subsequently contracted by means of the sequential diagonalization and truncation procedure, is $\{|X_\alpha^{\rm PO}\rangle|Y_\beta^{\rm PO}\rangle|Z_\gamma^{\rm PO}\rangle|jm\rangle|\varphi_v\rangle\}$. $\{|X_\alpha^{\rm PO}\rangle\}$, $\{|Y_\beta^{\rm PO}\rangle\}$, and $\{|Z_\gamma^{\rm PO}\rangle\}$ are 1D potential-optimized[29] (PO) discrete variable representations (DVRs) for x, y and z coordinates, respectively; they are labeled by the DVR grid points $\{X_\alpha\}$, $\{Y_\beta\}$, and $\{Z_\gamma\}$. The spherical harmonics $\{|jm\rangle\}$ constitute the angular (θ, ϕ) basis, while $\{|\varphi_v\rangle\}$ are the eigenfunctions of the diatomic vibrational Hamiltonian h_v:

$$h_v = -\frac{\hbar^2}{2\mu_d}\frac{\partial^2}{\partial r^2} + V_d(r). \tag{2}$$

In Eq. (2), μ_d is the reduced mass of the diatomic molecule, and $V_d(r)$ is a reference potential for the diatomic vibration, obtained by making a cut along r through the 6D PES for a large value of the molecule-surface distance R. The 1D PO-DVR bases were obtained as described in Ref. 18, using 1D reference potentials[18] V_0^x, V_0^y, and V_0^z. The reference potential in each Cartesian coordinate was defined by setting the other five coordinates in the 6D molecule–surface PES to their equilibrium values.

In the process of calculating the eigenstates of the 6D Hamiltonian in Eq. (1), as the first step of the diagonalization and truncation procedure a 3D eigenvalue problem is solved for each triplet of PO DVR points $(X_\alpha, Y_\beta, Z_\gamma)$, in the $\{|jm\rangle|\varphi_v\rangle\}$ basis:

$$^{\rm 3D}h^{\alpha\beta\gamma}|^{\rm 3D}\Phi_p^{\alpha\beta\gamma}\rangle = {}^{\rm 3D}\epsilon_p^{\alpha\beta\gamma}|^{\rm 3D}\Phi_p^{\alpha\beta\gamma}\rangle, \tag{3}$$

where

$$^{\rm 3D}h^{\alpha\beta\gamma} = -\frac{\hbar^2}{2\mu_d}\frac{\partial^2}{\partial r^2} + \frac{\mathbf{j}^2}{2\mu_d r^2} + V(X_\alpha, Y_\beta, Z_\gamma, r, \theta, \phi), \tag{4}$$

and

$$|^{\rm 3D}\Phi_p^{\alpha\beta\gamma}\rangle = \sum_{jmv} {}^{\rm 3D}C_{jmv,p}^{\alpha\beta\gamma}|jm\rangle|\varphi_v\rangle. \tag{5}$$

The Hamiltonian $^{\rm 3D}h^{\alpha\beta\gamma}$ in Eq. (4) describes the (hindered) rotation of the diatomic molecule coupled to its intramolecular vibration. The eigenstates $\{|^{\rm 3D}\Phi_p^{\alpha\beta\gamma}\rangle\}$ provide a quasiadiabatic 3D basis which is locally optimal for each 3D cut through the 6D PES, defined by $(X_\alpha, Y_\beta, Z_\gamma)$. At every 3D cut, only those eigenvectors $|^{\rm 3D}\Phi_p^{\alpha\beta\gamma}\rangle$ whose eigenvalues $^{\rm 3D}\epsilon_p^{\alpha\beta\gamma}$ are below the energy cutoff $^{\rm 3D}\epsilon_{\rm cut}$, are included in the 4D basis for the next cycle of the diagonalization and truncation procedure. In this cycle, for each pair of PO DVR points (X_α, Y_β), we solve a 4D eigenvalue problem in the $\{|Z_\gamma^{\rm PO}\rangle|^{\rm 3D}\Phi_p^{\alpha\beta\gamma}\rangle\}$ basis:

$$^{\rm 4D}h^{\alpha\beta}|^{\rm 4D}\Phi_q^{\alpha\beta}\rangle = {}^{\rm 4D}\epsilon_q^{\alpha\beta}|^{\rm 4D}\Phi_q^{\alpha\beta}\rangle, \tag{6}$$

where

$$^{\rm 4D}h^{\alpha\beta} = -\frac{\hbar^2}{2\mu}\frac{\partial^2}{\partial z^2} - \frac{\hbar^2}{2\mu_d}\frac{\partial^2}{\partial r^2} + \frac{j^2}{2\mu_d r^2} + V(X_\alpha, Y_3, z, r, \theta, \phi), \tag{7}$$

and

$$|^{\rm 4d}\Phi_q^{\alpha\beta}\rangle = \sum_{\gamma p} {}^{\rm 4D}C_{\gamma p,q}^{\alpha\beta}|Z_\gamma^{\rm PO}\rangle|^{\rm 3D}\Phi_p\rangle. \tag{8}$$

The 4D Hamiltonian in Eq. (7) couples the out-of-plane (z) motion of the diatomic's center of mass to the 3D Hamiltonian of Eq. (4). Again, only the 4D eigenvectors $|^{\rm 4D}\Phi_q^{\alpha\beta}\rangle$ with eigenvalues $^{\rm 4D}\epsilon_q^{\alpha\beta}$ smaller than the energy cutoff $^{\rm 4D}\epsilon_{\rm cut}$ are kept for the final 6D basis. In the last step, the matrix of the full 6D vibrational Hamiltonian in Eq. (1) is constructed in the contracted basis $\{|X_\alpha^{\rm PO}\rangle|Y_\beta^{\rm PO}\rangle|^{\rm 4D}\Phi_q\rangle\}$. As discussed earlier,[16] the dimension of the final contracted basis is about three orders-of-magnitude smaller than that of the primitive, uncontracted basis $\{|X_\alpha^{\rm PO}\rangle|Y_\beta^{\rm PO}\rangle|Z_\gamma^{\rm PO}\rangle|jm\rangle|\varphi_v\rangle\}$. Diagonalization of this Hamiltonian matrix yields the desired 6D vibrational energy levels and wave functions.

1. 6D calculations when the diatom stretching vibration is excited

The above computational procedure is very efficient when the calculations are confined to vibrational energy lev-

els well below the stretching fundamental of the diatomic molecule, the mode usually having by far the highest frequency. However, if one is interested in 6D vibrational eigenstates in which the diatom stretching vibration is excited, our computational scheme has to be modified. We illustrate this using CO/Cu(100) as an example. The CO stretch fundamental in this system is at $\approx$2079 cm^{-1}. When calculating the vibrational energy levels in the CO $v=1$ manifold, lying 2100 cm^{-1} or more above the ground state, the 3D and 4D energy cutoffs ${}^{3D}\epsilon_{cut}$ and ${}^{4D}\epsilon_{cut}$ must be set to much higher values than those needed for the ground CO stretch. This would produce prohibitively large intermediate 3D and 4D bases. However, it is possible to exploit the fact that because of the large energy gap between the ground and excited CO-stretch vibrational manifolds, the coupling between them is very weak. Consequently, one can truncate the intermediate 3D basis not just from above but also from *below*, by discarding those 3D eigenstates with eigenvalues significantly below the energy of the CO stretch fundamental. The discarded 3D eigenstates belong to the *ground* CO-stretch manifold and make a negligible contribution to the CO-stretch excited states. Such a truncation from *both* above and below, first implemented in the 6D calculations of HX-stretch excited HX dimers (X=F,Cl),[30–32] leaves only a narrow band of 3D eigenstates, typically 50–100 at each triplet of PO DVR points $(X_\alpha, Y_\beta, Z_\gamma)$, around the CO stretch fundamental, which are included in the 4D basis in which ${}^{4D}h^{\alpha\beta}$ of Eqs. (6) and (7) is diagonalized. Thanks to this scheme, the 6D calculations of CO-stretch excited vibrational eigenstates of the CO/Cu(100) system are no more demanding than those for ground CO stretch.

C. 5D treatments

In many cases, including CO/Cu(100), the frequency of the adsorbate stretching vibration is considerably higher than that of the the other, ''external'' molecular vibrations (frustrated rotations and translations). Under those circumstances, it is possible to treat this intramolecular vibration separately from the rest of the vibrational manifold, which significantly reduces the computational effort without introducing large errors. This can be done in two ways. One can simply freeze the diatomic bond length r at the equilibrium or averaged value, which eliminates the kinetic energy operator for the r coordinate from the 6D Hamiltonian in Eq. (1). Thus it becomes an effective 5D Hamiltonian, with the 5D potential $V^{5D}=V(x,y,z,r=r_{eq},\theta,\phi)$. The alternative which we prefer is to treat the diatomic stretching vibration diabatically, which essentially amounts to including only one diatomic vibrational state $|\varphi_v\rangle$ in 6D basis. The result is the effective 5D Hamiltonian H_v^{5D},

$$H_v^{5D}=-\frac{\hbar^2}{2\mu}\left(\frac{\partial^2}{\partial x^2}+\frac{\partial^2}{\partial y^2}+\frac{\partial^2}{\partial z^2}\right)+B_v\mathbf{j}^2 + V_v^{5D}(x,y,z,\theta,\phi), \tag{9}$$

where

$$B_v=\langle\varphi_v|\frac{1}{2\mu_d r^2}|\varphi_v\rangle, \tag{10}$$

and

$$V_v^{5D}=\langle\varphi_v|V(x,y,z,r,\theta,\phi)|\varphi_v\rangle. \tag{11}$$

Note that H_v^{5D} in Eq. (9), and therefore its energy levels, depend on the vibrational state v, ground or excited, of the molecule, since both V_v^{5D} and B_v involve averaging over its vibrational eigenstate $|\varphi_v\rangle$. Clearly, H_v^{5D} provides a measure of coupling between the diatomic stretching vibration and the ''external'' vibrational modes which is not present in the simpler frozen-diatom 5D teatment above, and is therefore employed in the 5D calculations reported in this article.

In addition, this formulation of the 5D treatment allows us to calculate the *shift* in the stretching frequency of the diatomic adsorbate from that of the molecule in the gas phase. The vibrational frequency shift $\Delta\nu$ (caused by adsorption) is obtained as[16–18]

$$\Delta\nu=E_{v=1}^0-E_{v=0}^0, \tag{12}$$

where $E_{v=1}^0$ and $E_{v=0}^0$ are the ground state energies of H_v^{5D} in Eq. (9) for the $v=1$ and $v=0$ states of the diatomic molecule, respectively. This expression was used by us earlier to calculate the vibrational frequency shifts of the HF molecule in argon clusters.[16–18,33]

D. 4D fixed-site treatment

In the course of the present work, we also performed 4D calculations in which the lateral coordinates (x,y) of the center of mass of the diatom are fixed at values (x_0,y_0) of the binding site considered, while the remaining four degrees of freedom (z,r,θ,ϕ) are treated explicitly, as fully coupled. This approximation removes the kinetic energy operators for the x and y coordinates from the 6D Hamiltonian in Eq. (1), resulting in the following 4D Hamiltonian:

$$H^{4D}=-\frac{\hbar^2}{2\mu}\frac{\partial^2}{\partial z^2}-\frac{\hbar^2}{2\mu_d}\frac{\partial^2}{\partial r^2}+\frac{\mathbf{j}^2}{2\mu_d r^2} + V(x=x_0,y=y_0,z,r,\theta,\phi). \tag{13}$$

We point out that H^{4D} in Eq. (13) is identical to the intermediate Hamiltonian ${}^{4D}h^{\alpha\beta}$ of Eq. (7) in the sequential diagonalization and truncation procedure. The calculations reported in this article using H^{4D} will be referred to as the fixed-site calculations. This Hamiltonian was employed in recent 4D quantum dynamical investigations of the dissociative adsorption of diatomic molecules on rigid surfaces.[34]

Obviously, the lateral, in-plane vibrational dynamics of the adsorbed diatom is left out from the 4D fixed-site bound state treatment. While this is a serious limitation, at the same time it provides the main rationale for performing such bound state calculations. Comparison of the 4D fixed-site results to those of higher-dimensional 5D and 6D treatments provides information regarding the strength of coupling between the in-plane motions (frustrated translation) of the adsorbate and other vibrational modes, and how it affects the accuracy of the calculated vibrational eigenstates.

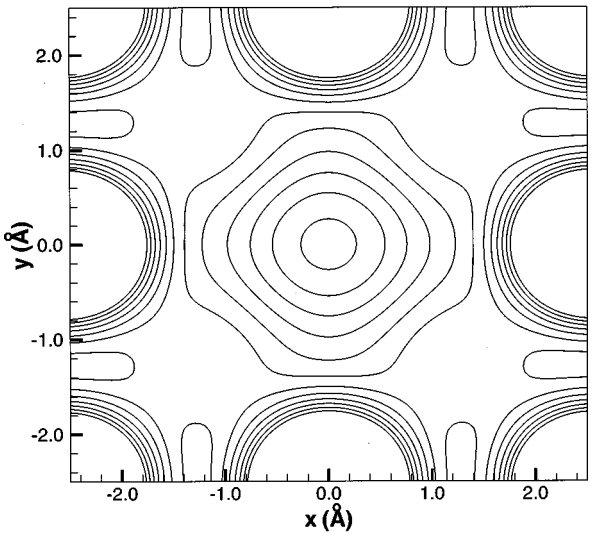

FIG. 2. Contour plot of the 6D PES for CO/Cu(100) used in the calculations. The CO molecule is bound at the on-top site in the center of the plot, while the other sites are unoccupied. Potential cut in the *xy* plane is shown, for $z=2.20$ Å, $\theta=180°$, $\phi=0°$, $r=1.126$ Å. The first contour is drawn at -4600 cm^{-1}, and the energy spacing between the subsequent contours is 400 cm^{-1}.

III. COMPUTATIONAL ASPECTS

The CO/Cu(100) PES employed in our calculations is due to Tully and co-workers.[13,14] It is an empirical potential, in which the CO molecule interacts with a $6\times6\times3$ slab of copper atoms. The gas–surface interaction potential is additive over all Cu atoms; it consists of a CO–Cu interaction which depends both on the Cu–C separation and the angle between O–C and C–Cu bonds, plus a gas-phase Morse potential for CO. For this potential, the minimum energy configuration corresponds to CO bound via the carbon end, perpendicular to the surface on top of a single Cu atom, in agreement with experiment. Prior to the bound state calculations we optimized the CO–Cu geometry, just as Bowman *et al.*[5,6] in their VSCF calculations. The energy minimization included the coordinates of the CO molecule and the Cu atom to which CO is bound, while all other Cu atoms were held fixed in their equilibrium positions. In the optimized geometry, the C–Cu distance is 1.909 Å, the C–O bond length is 1.126 Å, and the Cu atom bonded to CO is 0.352 Å below the copper surface. Contour plot of the lateral (x,y) portion of this PES is shown in Fig. 2.

As discussed in Sec. II A, in the RS calculations the reduced mass μ appearing in Eq. (1) was set equal to the mass of CO molecule, $\mu=M_{\mathrm{CO}}=28.01$ amu. In the calculations employing the SM model also presented in Sec. II A, μ was defined as $\mu_{\mathrm{CO/Cu}}=M_{\mathrm{CO}}M_{\mathrm{Cu-atom}}/(M_{\mathrm{CO}}+M_{\mathrm{Cu-atom}})=19.44$ amu. $M_{\mathrm{Cu-atom}}=63.55$ amu is the mass of the single Cu atom to which the CO molecule is bound (it is the average mass of the two Cu isotopes, weighted by their abundance).

The PO DVRs for x, y and z coordinates $\{|X_\alpha^{\mathrm{PO}}\rangle|Y_\beta^{\mathrm{PO}}\rangle|Z_\gamma^{\mathrm{PO}}\rangle\}$ were generated using the 1D sine DVRs of Colbert and Miller.[35] Thirty sine-DVR grid points were distributed over the range $-1.2\,\text{Å}\leqslant\lambda\leqslant1.2\,\text{Å}$, where $\lambda=x,y$. In the z direction, 60 sine-DVR grid points were used in the range $1.0\,\text{Å}\leqslant z\leqslant3.4\,\text{Å}$. The dimensions of the 1D PO DVRs in x,y,z were $N_x^{\mathrm{PO}}=N_y^{\mathrm{PO}}=11$ and $N_z^{\mathrm{PO}}=9$. The angular basis $\{|jm\rangle\}$ included functions up to $j_{\max}=30$. The initial 6D basis for the ground CO-stretch calculations included CO $v=0,1$ eigenstates, and the CO $v=2$ eigenstate was added to the basis for the excited CO-stretch calculations. The energy cutoffs were set to ${}^{3\mathrm{D}}\epsilon_{\mathrm{cut}}=3000\,\mathrm{cm}^{-1}$ and ${}^{4\mathrm{D}}\epsilon_{\mathrm{cut}}=2000\,\mathrm{cm}^{-1}$ for ground CO-stretch calculations, and to ${}^{3\mathrm{D}}\epsilon_{\mathrm{cut}}=4000\,\mathrm{cm}^{-1}$ and ${}^{4\mathrm{D}}\epsilon_{\mathrm{cut}}=3500\,\mathrm{cm}^{-1}$ for excited CO-stretch calculations. In addition, in the excited CO-stretch calculations, at each triplet of PO DVR points $(X_\alpha,Y_\beta,Z_\gamma)$, 50 3D eigenstates $|{}^{3\mathrm{D}}\Phi_p^{\alpha\beta\gamma}\rangle$ above that corresponding to CO $v=1$ and five 3D eigenstates below it were included in the 4D basis. The dimensions of the final 6D matrices of the full Hamiltonian in Eq. (1) for the ground and excited CO-stretch calculations were 2062 and 2200, respectively.

IV. RESULTS AND DISCUSSION

Table I gives the fundamental frequencies of the six molecular vibrational modes of $^{12}C^{16}O$/Cu(100), from our 4D,

TABLE I. Calculated and measured frequencies (in cm^{-1}) of the vibrational fundamentals of $^{12}C^{16}O$ on Cu(100).

	5D[a]		4D (on-top site)[b]		6D[c]	VSCF			
Mode	RS[d]	SM[e]	RS[d]	SM[e]	SM[e]	9D+CI[g]	9D[h]	6D[i]	Experiment[j]
Frust. trans.	22.4	27.6	⋯	⋯	27.3	24	33.7	31.6	31.7
Frust. rot.	332.5	333.5	328.7	328.0	333.3	340	361.0	353.8	287.2
CO–Cu stretch	293.8	351.2	291.9	349.4	347.5	348	346.5	349.3	344.6
CO stretch	2146.3[f]	2146.2[f]	2152.4	2153.1	2153.5	2154	2133.0	2129.1	2079

[a]Present work. The 5D treatment is described in Sec. II C.
[b]Present work. The 4D fixed-site treatment is described in Sec. II D.
[c]Present work. The 6D treatment is described in Sec. II A.
[d]Rigid-surface (RS) model. $\mu=M_{\mathrm{CO}}=28.01$ amu, see Secs. II A and III.
[e]Surface-mass (SM) model. $\mu_{\mathrm{CO/Cu}}=M_{\mathrm{CO}}M_{\mathrm{Cu-atom}}/(M_{\mathrm{CO}}+M_{\mathrm{Cu-atom}})=19.44$ amu, see Secs. II A and III.
[f]Calculated using Eq. (12), as described in Sec. IV.
[g]9D VSCF+CI, Ref. 36.
[h]Reference 6.
[i]Reference 5.
[j]References 10–12.

5D, and 6D calculations, and from several VSCF calculations by Bowman and co-workers.[5,6,36] Also shown are the experimental results.[11,12]

The 5D frequencies of the CO stretch fundamental listed in Table I were obtained by calculating the frequency shift $\Delta\nu$ using Eq. (12). The ground-state energies $E^0_{\nu=1}$ and $E^0_{\nu=0}$ of H^{5D}_ν in Eq. (9) were found to be -4176.0 and -4191.6 cm^{-1}, respectively, giving $\Delta\nu = 15.6\,cm^{-1}$. This frequency shift was added to the calculated stretching frequency of isolated CO on this PES, 2130.6 cm^{-1}, yielding the (5D) CO stretch fundamental at 2146.2 cm^{-1}.

A. Comparison of the surface-mass and the rigid-surface model results

We begin by discussing how the choice of the reduced mass μ in the Hamiltonian in Eq. (1) affects the calculated fundamental frequencies, by comparing the 5D results from the RS ($\mu = M_{CO}$) and SM ($\mu_{CO/Cu}$) model calculations. From Table I it is evident that the modes most sensitive to the choice of μ are those consisting primarily of the motion of the center of mass of CO, the in-plane doubly degenerate frustrated translation and the out-of-plane CO–Cu stretch. Replacing $\mu = M_{CO} = 28.01$ amu with $\mu_{CO/Cu} = 19.44$ amu increases the fundamental frequency of the frustrated translation mode by 21.9% and that of the CO–Cu stretch by 19.5%. In contrast, the frequencies of the fundamentals of the doubly degenerate frustrated rotation and the CO stretch modes are virtually the *same* for *both* values of μ. The same trend is present in the results of the 4D fixed-site calculations, which do not include the lateral (x,y) dynamics but which explicitly couple the CO stretching vibration to the other two external modes considered.

The pronounced μ-dependence of the frustrated translation and the CO–Cu stretch modes is not surprising. In Eq. (1), μ appears only in the kinetic energy (KE) operator for the Cartesian coordinates x, y (mainly parallel frustrated translation) and z (mainly CO–Cu stretch), and not in the KE operators for the diatomic stretching coordinate r or the diatom rotation (the $\mathbf{j}^2$ term). This explains the insensitivity of the CO stretch and frustrated rotation modes to the value of μ.

The physical significance of accounting for the surface atom motion as done in the SM model becomes apparent when the fundamental frequencies of the frustrated rotation and CO–Cu stretch modes calculated in 5D and 4D using the RS and SM models are compared to experimental values. One sees that the RS calculations, both 5D and 4D, give a higher fundamental frequency for the frustrated rotation mode than for the CO–Cu stretch mode, which is *opposite* to experimental observation. However, the SM model treatment in 5D and 4D, in which the reduced mass μ takes into account the Cu atom directly bonded to CO, predict that the CO–Cu stretch fundamental is higher in energy than the frustrated rotation fundamental, *in accord* with experiment. This reversal in the energy ordering of the fundamentals of the two modes is caused by the fact pointed out earlier, that the replacement of $\mu = M_{CO}$ (RS model) with $\mu_{CO/Cu}$ (SM model) leads to a 20% increase in the frequency of the CO–Cu stretch fundamental, putting it above the frustrated rotation fundamental whose frequency remains practically unchanged. More quantitative comparison between our calculations and experiment is made in Sec. IV C.

B. Comparison to VSCF calculations

Our confidence in the basic correctness of the results obtained with the SM model was increased by the comparison of the fundamentals from the 6D SM model calculations to those from the 6D and 9D VSCF calculations by Bowman and co-workers[5,6] on the same PES, shown in Table I. The 6D VSCF results[5] in Table I put the frustrated rotation fundamental above the CO–Cu stretch fundamental, in contradiction to experiment (just as our 5D and 4D RS calculations). This feature persists in the 9D VSCF results[6] shown in Table I. This was puzzling since, based on our SM model calculations, we expected that inclusion of the Cu–atom motion in the 9D VSCF calculations would reverse the ordering of the two fundamentals. The fact that it did not, could lead one to conclude that (i) this (incorrect) ordering simply reflects a defficiency of the PES employed, and (ii) the (correct) ordering predicted by the 5D and 4D SM model calculations for this PES is actually an artifact of the model.

However, recent recalculation by Bowman,[36] in which the configuration interaction (CI) was added to the 9D VSCF, did reverse the ordering of the frustrated rotation and CO–Cu stretch fundamentals which emerged from the 9D (and 6D) VSCF calculations without the CI,[6] thereby bringing the VSCF results in much closer agreement with our 6D SM model calculations. In the following, we refer to the 9D VSCF+CI as 9D+CI. Particularly important for establishing the level of accuracy of the 6D SM model treatment is the comparison of the frustrated translation and the CO–Cu stretch fundamentals, for which the SM and RS model yield rather different frequencies, to those from the 9D+CI calculations.[36] The 6D SM CO–Cu stretch fundamental and its 9D+CI counterpart have virtually identical frequencies (which are ≈ 50 cm^{-1} higher than the 6D RS value), providing strong evidence for the validity and accuracy of the SM model. For the frustrated translation fundamental the 6D SM and 9D+CI results differ by 12%. The slightly worse agreement is probably due to two factors: (i) Accurate description of this very-low-frequency mode presents difficulties for the VSCF treatment, as evidenced by the large correction (29%) which the CI makes to the 9D VSCF result. In sharp contrast, the frequencies of the CO–Cu stretch fundamental from the 9D+CI and 9D VSCF calculations differ by only 0.4%. (ii) The SM model introduces some error in the calculated frustrated translation fundamental. It is not possible for us to estimate at this time the relative importance of (i) and (ii).

Our 6D SM frustrated rotation fundamental and that from the 9D+CI calculations agree very well, to within 2%. In this case, we have two reasons to believe that this small discrepancy can be attributed mostly to the VSCF treatment: (i) As discussed earlier, the RS and SM model calculations give fundamental frequencies for the frustrated rotation which are practically the same (≈ 1 cm^{-1} apart), showing that the effects due to the surface-atom mass are negligible for this mode. This implies very weak coupling of surface vibrations to the frustrated rotation, so that the fundamental

TABLE II. Comparison of isotopic frequency shifts (in cm^{-1}) of the vibrational fundamentals relative to the frequencies for $^{12}C^{16}O$ from the SD surface-mass model calculations in this work (theory) and experiment (Ref. 11), given in Table I.

	$^{13}C^{16}O$		$^{12}C^{18}O$		$^{13}C^{18}O$	
Mode	Theory	Exp.	Theory	Exp.	Theory	Exp.
Frust. trans.	−0.5	−0.3 (−0.7%)	−1.3	−1.5 (−4.4%)	−1.4	−1.6 (−4.9%)
Frust. rot.	−7.1	−8.9 (−3.1%)	−2.7	−2.8 (−1.0%)	−11.7	−11.3 (−3.9%)
CO–Cu stretch	−3.9	−3.3 (−1.0%)	−8.2	−7.2 (−2.1%)	−11.4	−10.5 (−3.0%)

frequency of the latter cannot be affected much by the level of the treatment of the adsorbate–substrate vibrational coupling. (ii) On the other hand, the 9D VSCF and 9D+CI calculations give considerably different fundamental frequencies (21 cm^{-1} apart), indicating fairly strong sensitivity to the level of the SCF treatment.

For the high-frequency CO stretch fundamental, the 6D SM and 9D+CI calculations give almost identical frequencies. Interestingly, such excellent agreement was achieved only after the CI correction of 21 cm^{-1} to the 9D VSCF result.

The above comparison to the 9D+CI results of Bowman[36] allows us to conclude that the 6D SM model calculations give highly accurate vibrational fundamentals of the CO/Cu(100) PES employed. We believe that a more rigorous treatment of the coupling between the diatom and substrate vibrations, beyond the SM model, will change the frequencies of the frustrated rotation and CO–Cu stretch fundamentals calculated for the *same* PES by no more than 2%–3%, and much less in the case of the CO stretch fundamental. The only exception to this low error estimate is the frustrated translation fundamental, where the uncertainty of the 6D SM model result should be about 10%.

C. Comparison to measured fundamental frequencies

We now proceed by comparing the result of the 6D SM model calculations to experimental data. The agreement is clearly the best for the CO–Cu stretch fundamental, the difference between theory (6D SM and 9D+CI) and experiment being just 0.7%. The agreement is less impressive for the frustrated rotation fundamental, whose 6D SM frequency is 16% higher than the experimental value. For reasons given in Sec. IV B, one can be virtually certain that this difference is due to a defficiency of the PES, as concluded earlier by Park *et al.*[5] The fundamental frequency of the frustrated translation mode from the 6D SM model calculations is 14% lower than the experimental result. Unfortunately, this difference is only slightly larger than the uncertainty which the SM model was estimated (in Sec. IV B) to introduce in the calculated frustrated translation fundamental. Consequently, we cannot say with confidence how much of the discrepancy between theory and experiment for this mode originates in the PES, and how much is due to the shortcomings of the SM-model treatment of the frustrated translation mode, in light of the discussion in Sec. II A.

The most significant discrepancy between the calculated and measured fundamental frequencies occurs for the CO stretch mode. The calculated frequency of 2153.5 cm^{-1} is 22.9 cm^{-1} *higher* than that which the PES gives for isolated CO molecule, 2130.6 cm^{-1}. This is in *qualitative discord* with experimental observation that the CO stretch fundamental for CO/Cu(100), at 2079 cm^{-1}, is 64 cm^{-1} *lower* than the stretching fundamental of gas-phase CO. In other words, theory predicts a *blue shift* of 22.9 cm^{-1} from the (theoretical) gas-phase CO stretch frequency, whereas experiment gives a *red shift* of 64 cm^{-1}. Since all bound-state calculations (6D SM, 4D SM and RS, 9D+CI) give the same CO stretch fundamental and thus the blue shift, we can be certain that this disagreement with experiment can be entirely attributed to the PES. Evidently, this PES[13,14] does not describe correctly the interaction between the C–O stretching coordinate and other degrees of freedom of CO/Cu(100).

It is of interest to discuss in this context the results of the normal-mode calculations by Lewis and Rappe[1,2] for a half-monolayer of CO molecules on Cu(100), referred to in the Introduction and Sec. II A, although a different potential was employed in these investigations. By solving a 1D Schrödinger equation for a quartic anharmonic potential along a frustrated translation coordinate the frequency of 27 cm^{-1} was obtained,[2] in excellent agreement with the 6D SM frustrated translation fundamental in Table I, 27.3 cm^{-1}, and close to the experimental value of 32 cm^{-1}. Their frequency of the frustrated rotation fundamental, 282 cm^{-1}, is closer to the experimental result of 287 cm^{-1} than our 6D SM value, 333 cm^{-1}. But, the situation reverses for the CO–Cu stretch fundamental; the 6D SM frequency, 348 cm^{-1}, agrees much better with the measured value of 345 cm^{-1} than the result of Lewis and Rappe,[2] 427 cm^{-1}.

D. Calculated and observed isotope shifts of the fundamental frequencies

Graham *et al.*[11] have measured the fundamental frequencies of the external modes of CO at the on-top sites on Cu(100) for all for isotopomers of CO, $^{12}C^{16}O$, $^{13}C^{16}O$, $^{12}C^{18}O$, and $^{13}C^{18}O$. This motivated us to perform the 6D SM model calculations for $^{13}C^{16}O$, $^{12}C^{18}O$, and $^{13}C^{18}O$, in addition to those for $^{12}C^{16}O$ discussed above. The theoretical and experimental results are presented in Table II, as shifts from the theoretical (6D SM) and experimental fundamentals for $^{12}C^{16}O$ given in Table I. It is clear from Table II that very good agreement exists between the calculated and measured isotope shifts of the frequencies of the three external modes.

It was noted by Graham *et al.*[11] that, as evident from Table II, the fundamental frequency of the frustrated translation mode shifts considerably more upon isotopic substitution of the oxygen atom than carbon, whereas the isotope

shift of the frustrated rotation mode is larger when the carbon atom is exchanged. Our 6D SM model calculations quantitatively reproduce these experimental observations. As already discussed,[11] these isotope shifts indicate significant coupling between the translational and rotational motions of the adsorbed CO molecule. Stronger dependence of the frustrated translation frequency on the oxygen mass implies an appreciable tilting motion of the O atom and a smaller vibrational amplitude of the C atom. The implication is that this mode looks more like a ''wagging'' motion of the CO molecule about the surface Cu atom, than an in-plane translation of the CO center-of-mass.[11]

E. Comparison of the results of 4D, 5D, and 6D calculations

Comparing the results of lower-dimensional 4D and 5D calculations to those obtained using the 6D treatment can shed light on the strength of couplings between different vibrational modes, and how they reflect in the energy level structure of the CO/Cu(100) system.

Table I shows that the fundamental frequencies of the external modes from the 5D (fixed CO bond length) and 6D SM model calculations are virtually identical; only in the case of the CO–Cu stretch there is a difference of 1%. The implication is that the coupling of the CO stretch mode to other vibrations in the system is very weak on this PES, which is not surprising in view of at least a factor of six difference between the CO stretch fundamental and other fundamental frequencies. Thus, the 5D treatment described in Sec. II C can be used to study the quantum dynamics of the external vibrations of CO/Cu(100), with little loss of accuracy. Even the frequency shift Δv of the CO stretch fundamental from the 5D calculations [15.6 cm^{-1}, using Eq. (12)] agrees well with the 6D frequency shift of 22.9 cm^{-1}.

More surprising is the comparison between the 4D fixed-site SM results and the 6D SM fundamental frequencies. In the 4D calculations, described in Sec. II D, the lateral coordinates of the CO center of mass (COM) were fixed at $x=y=0$, corresponding to CO at the minimum-energy on-top site. Thus the COM cannot move parallel to the surface. Despite this drastic restriction on the COM motion, the fundamentals from the 4D SM treatment agree surprisingly well with those from the 6D SM calculations. For the frustrated rotation and CO–Cu stretch fundamentals the differences are only 1.6% and 0.5%, respectively, and for the CO stretch fundamental the difference between the 4D and 6D frequencies is indeed negligible, 0.4 cm^{-1}. The fact that freezing the lateral COM motion has such a small effect on other modes tells us that the frustrated translation mode is almost decoupled from other external and internal vibrations of CO on Cu(100). This must be due to the very large frequency mismatch (one order of magnitude or more) between the frustrated translation fundamental and other fundamentals.

The CO/Cu(100) system is by no means unique in this respect. Fundamental frequencies of the frustrated translation mode measured for CO on Ni(100) and Pt(111) are below 50 cm^{-1}, and are an order of magnitude smaller than the frequency of the respective CO–metal stretch mode.[10] This suggests that the 4D fixed-site treatment would be applicable to these and other similar systems. It could be used in preliminary testing or screening of PESs, as a low-cost alternative to the 6D calculations (of course, no information would be gained about the in-plane portion of the PESs).

F. Analysis of excited energy levels of the frustrated translation mode

The doubly degenerate frustrated translation mode has received a great deal of attention in the past decade.[10,11,37–39] As by far the lowest energy mode of the CO/Cu(100) system, it is thermally excited already at low temperatures (below the CO desorption temperature of $T_{des} \approx 160$ K), unlike the higher-energy external modes.[10] For this reason, it plays a key role in the low-temperature vibrational dynamics of CO/Cu(100). Its vibrational amplitude parallel to the surface is relatively large (see below) and therefore this mode is an important source of information about the lateral adsorbate–substrate potential. Furthermore, it is directly involved in the surface diffusion and, because of its low frequency, provides an efficient energy pathway for the vibrational relaxation of the excited CO stretch and CO–Cu stretching modes to the phonons of the substrate.[3,4]

Clearly, it is of interest to analyze the assignment and the level structure of the excited states of the frustrated translation mode. The 15 lowest vibrational levels from the 6D SM calculations are displayed in Table III. They are labeled by the irreducible representations (IRs) of C_{4v} point group. Also shown for each level are the root-mean-square (RMS) amplitudes (displacements) of the vibrations, $\Delta x, \Delta y, \Delta z$, along the three Cartesian axes. In the case of doubly degenerate states of *e* symmetry, the RMS amplitudes are given for only one member of the pair. For the second (orthogonal) component, $\Delta x^{(2)} = \Delta y^{(1)}$, and $\Delta y^{(2)} = \Delta x^{(1)}$, where (1) and (2) label the two members of the degenerate pair. In this energy range only the frustrated translation mode can be excited. All other (molecular) modes of CO/Cu(100) are in the ground state. Consequently, only two (nonzero) quantum numbers are needed to assign the 6D vibrational levels shown in Table III. The assignment of the excited states of the 2D frustrated translation mode can be attempted using two sets of quantum numbers. One set is $[v_x, v_y]$, where v_x and v_y denote the number of quanta in the (approximate) 1D Cartesian vibrational modes along the *x* and *y* axis, respectively. Alternatively, since the vibrations in the *x* and *y* directions are degenerate (due to high symmetry of the PES), it may be appropriate to use also the quantum numbers (v,l) of the 2D isotropic oscillator, where v denotes the number of quanta in the frustrated translation mode, while the quantum number l characterizes the vibrational angular momentum around the $C_4(z)$ axis. For a given v, l can have $v+1$ values $-v, -v+2, ..., v-4, v-2, v$.[40] Which of these two sets of quantum numbers should be used for assigning a particular state is dictated by the appearance and symmetry of the nodal pattern evident in the 2D *xy* cuts through the 6D wave function. The quantum numbers $[v_x, v_y]$ or (v,l) are determined either by counting the number of nodes along *x* and *y* (for v_x, v_y), or by counting the number of angular nodes (for *l*, when the *xy* cut reveals cylindrical symmetry).

TABLE III. Low-lying excited vibrational levels of $^{12}C^{16}O$/Cu(100) from 6D SM calculations. ΔE (in cm^{-1}) stands for the difference $E-E_0$, with the ground-state energy $E_0=-4194.34\ cm^{-1}$. Root-mean-square amplitudes Δx, Δy, Δz are in Å. The levels are labeled using the irreducible representations of C_{4v} point group. $\mathcal{N}$ denotes the number of quanta in the frustrated translation mode. The quantum numbers (v,l) and $[v_x,v_y]$ for the doubly degenerate frustrated translation mode are defined in Sec. IV F. All other vibrational modes of CO/Cu(100) considered are unexcited in this energy range, and their quantum numbers (zero) are not shown.

n	ΔE	Δx	Δy	Δz	Symmetry	$\mathcal{N}$	(v,l) or $[v_x,v_y]$
0	0.00	0.17	0.17	0.05	a_1	0	(0,0)
1/2	27.33	0.19	0.28	0.05	e	1	(1,1)
3	54.82	0.29	0.29	0.05	b_2	2	(2,2)
4	59.20	0.27	0.27	0.05	b_1	2	(2,2)
5	59.23	0.27	0.27	0.05	a_1	2	(2,0)
6/7	86.91	0.34	0.29	0.05	e	3	[2,1]/[1,2]
8/9	97.03	0.33	0.23	0.05	e	3	[3,0]/[0,3]
10	119.27	0.34	0.34	0.05	a_1	4	[2,2]
11	124.73	0.33	0.33	0.05	a_2	4	(4,4)
12	125.04	0.32	0.32	0.05	b_2	4	(4,2)
13	143.71	0.28	0.28	0.05	b_1	4	(4,2)
14	143.77	0.28	0.28	0.05	a_1	4	(4,0)

Figures 3–6 show the *xy* cuts through the 6D wave functions of the states $n=0-14$ listed in Table III. A third quantum number, $v_z(=0)$ appears in the labels of the wave function plots; it denotes the number of quanta (zero) in the vibration along the *z*-axis (mainly CO–Cu stretch). The assignments in Table III are based on these wave function plots. The majority of states were assigned with the quantum numbers (v,l), but in some cases Cartesian quantum numbers $[v_x,v_y]$ were required. We encountered this type of switching between (v,l) and $[v_x,v_y]$ quantum numbers in our earlier investigations of the intermolecular vibrations in atom-large molecule complexes *o*–xylene–Ar (Ref. 41) and 2,3-dimethylnaphthalene–He.[27] The wave functions and their nodes revealed by the *xy* cuts in Figs. 3–6 are highly regular, apparently undistorted by coupling to other vibrational degrees of freedom. This provides additional evidence for very weak coupling between the frustrated translation mode and other vibrational modes of CO/Cu(100), suggested in Sec. IV E on the basis of excellent agreement between the fundamentals from the 4D fixed-site calculations and 6D calculations. Finally, we note that the (v,l) levels in Table III which have same v but different l values have different energies. This reflects the anharmonicity of the lateral potential; if the frustrated translation mode were a *harmonic* 2D isotropic oscillator, its energy levels would *not* depend on l but only on v.

Table III exhibits a rather conspicuous and intriguing pattern: the $\mathcal{N}+1$ vibrational levels with *odd* number of quanta $\mathcal{N}$ are grouped into pairs of *exactly* degenerate states, one pair for $\mathcal{N}=1$ and two pairs for $\mathcal{N}=3$, while the levels with *even* $\mathcal{N}$ display no such degeneracy. Instead, for $\mathcal{N}=2$, two levels are *almost* degenerate and the third level has appreciably lower energy, while for $\mathcal{N}=4$, four levels appear as two pairs of *almost* degenerate states and the unpaired fifth level lies below the two pairs. It turned out that this pattern can be qualitatively understood with the help of group theory. The argument which follows is rigorously valid for harmonic vibrations but, as we shall see, its conclusions are in full accord with the calculations. The $\mathcal{N}+1$ states which arise when $\mathcal{N}$ quanta are put in a doubly degen-

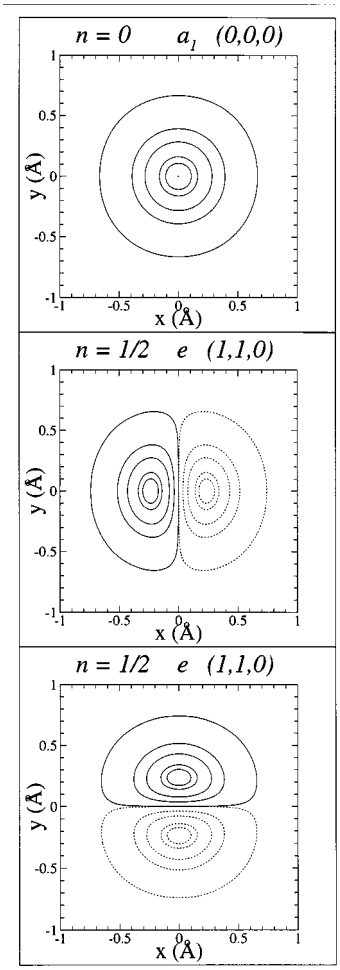

FIG. 3. Cuts in the *xy* plane through the 6D wave functions of the states $n=0$ ($\mathcal{N}=0$) and $n=1/2$ ($\mathcal{N}=1$) in Table III, for $z=2.55$ Å, $\theta=180°$, $\phi=0°$, $r=1.126$ Å. $\mathcal{N}$ denotes the number of quanta in the frustrated translation mode. Contours are for 99%, 80%, 50%, 25%, and 1% of the maximum amplitude for the respective cuts. Solid (dashed) curves enclose regions of positive (negative) amplitude.

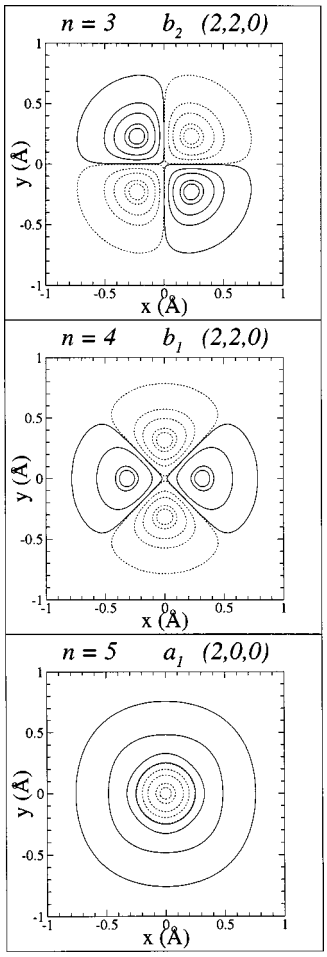

FIG. 4. Cuts in the *xy* plane through the 6D wave functions of the $\mathcal{N}=2$ states $n=3,4,5$ in Table III. For additional information, see Fig. 3.

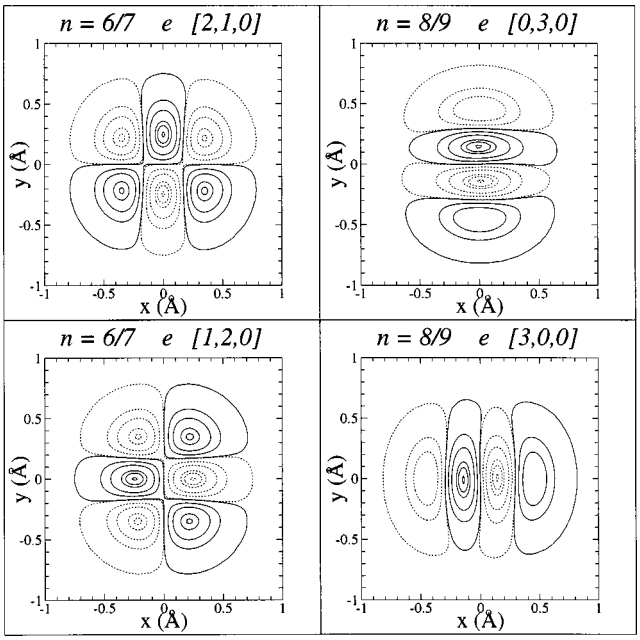

FIG. 5. Cuts in the *xy* plane through the 6D wave functions of the $\mathcal{N}=3$ states $n=6/7$ and $n=8/9$ in Table III. For additional information, see Fig. 3.

erate frustrated mode form the basis for a reducible representation of C_{4v} point group. Using standard group-theoretical techniques,[42] this reducible representation can be decomposed into the IRs of C_{4v} point group. For $\mathcal{N}=1-6$, the results are shown in Table IV. One can see that for *odd* $\mathcal{N}$, the reducible representation of dimension $\mathcal{N}+1$ decomposes into $(\mathcal{N}+1)/2$ two-dimensional IRs of type *E*. In contrast, when $\mathcal{N}$ is *even*, only one-dimensional IRs of C_{4v} point group (A_1,A_2,B_1,B_2) appear in the decomposition of the reducible representation. Thus, group theory predicts that odd-$\mathcal{N}$ levels would form pairs of degenerate states, as is indeed the case for the levels appearing in Table III. For the even-$\mathcal{N}$ levels, the group theory predicts that they belong eclusively to one-dimensional IRs, so that only accidental (near) degeneracies may occur. Again, this is exactly what one sees in Table III. It is gratifying to find that the level structure of the excitations of the (anharmonic) doubly degenerate frustrated translation mode which emerged from the quantum 6D calculations can be qualitatively accounted for by a simple group-theoretical treatment developed for harmonic degenerate vibrations.[42]

V. CONCLUSIONS

We have presented a computational methodology for exact quantum 6D calculations of the vibrational levels of a diatomic molecule adsorbed on a rigid corrugated surface. Apart from the static-surface assumption, this method is free from dynamical approximations and provides vibrational eigenstates which are numerically exact for the 6D PES employed. While the method is applicable to vibrations of any diatomic adsorbate, it is particularly advantageous in cases when the adsorbed molecule executes coupled, strongly anharmonic large-amplitude vibrations. Our methodology can be applied to molecules at adsorption sites with arbitrary geometry, such as surface steps and defects, and irregularly shaped clusters.

The 6D approach to adsorbate vibrations described here is completely rigorous in the rigid surface (RS) limit. Surface nonrigidity was introduced in a limited way, along the lines of the very simple surface-mass (SM) model,[9] by modifying the diatom-surface reduced mass to reflect the mass of the surface atom directly bound to the adsorbate. Comparison of RS and SM calculations for CO/Cu(100) showed that the modes most sensitive to changes of the reduced mass are the out-of-plane CO–Cu stretch and the in-plane (doubly degenerate) frustrated translation. Only the SM model calculations gave the energy ordering of the CO–Cu stretch and the frustrated rotation fundamentals in agreement with experiment.

The quantum 6D SM calculations of the vibrations of CO on Cu(100) were performed for all four isotopomers of CO, using the empirical potential by Tully and co-workers.[13,14] Our 6D SM fundamental frequencies for $^{12}C^{16}O$ are in very good agreement with those from the most recent 9D 9DVSCF+CI calculations by Bowman[36] on the same PES. The overall agreement with the measured frequencies of the $^{12}C^{16}O$ vibrational fundamentals is remarkably good given the empirical nature of the PES. Somewhat less well reproduced is the measured frequency of the frustrated rotation fundamental, where the 6D SM result is 16% higher than the experimental value, suggesting a deficiency

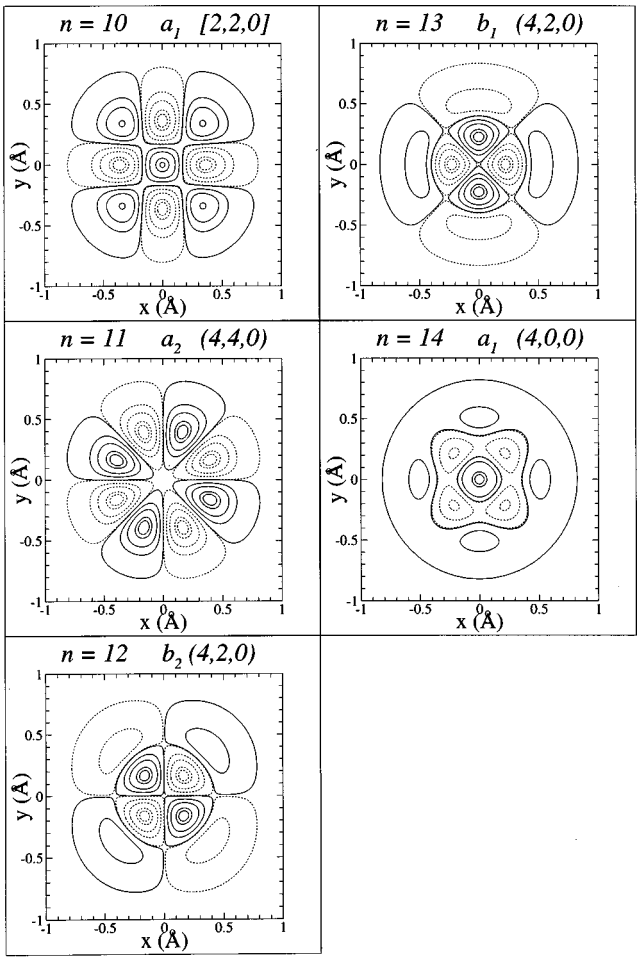

FIG. 6. Cuts in the *xy* plane through the 6D wave functions of the $\mathcal{N}=4$ states $n=10-14$ in Table III. For additional information, see Fig. 3.

in the angular anisotropy of the PES. Theory and experiment are in most serious disagreement regarding the CO stretch fundamental frequency. Our 6D treatment predicts a blue shift of 23 cm^{-1} relative to the gas-phase CO stretch frequency for this PES, whereas experimentally a red shift of 64 cm^{-1} is observed. The 9D VSCF+CI calculations of Bowman[36] give the same result. Therefore, we conclude that the PES employed does not describe correctly the coupling between the C–O stretching vibration and other degrees of freedom of CO/Cu(100). The 6D SM model calculations reproduce very well the isotope shifts of the fundamental frequencies of external CO modes (relative to $^{12}C^{16}O$) measured for $^{13}C^{16}O$, $^{12}C^{18}O$, and $^{13}C^{18}O$.

TABLE IV. Decomposition of the reducible representations with dimension $D_{\mathcal{N}}$ in terms of the irredicuble representations of C_{4v} point group. The reducible representations are formed in the basis of $\mathcal{N}+1$ states of the doubly degenerate frustrated translation mode which have $\mathcal{N}$ vibrational quanta.

$\mathcal{N}$	$D_{\mathcal{N}}$	Irreps.
1	2	E
2	3	$A_1+B_1+B_2$
3	4	$2E$
4	5	$2A_1+A_2+B_1+B_2$
5	6	$3E$
6	7	$2A_1+A_2+2B_1+2B_2$

Besides the 6D calculations reduced-dimensional 5D (rigid CO) and 4D (fixed-site) model calculations were performed, to gain insight in the couplings among the molecular modes of the adsorbed CO molecule. These calculations demonstrated that the CO stretch is coupled very weakly to the external CO modes. A bit more unexpected was the finding from the 4D fixed-site calculations, in which the CO molecule cannot move laterally, parallel to the copper surface. The fundamentals from the 4D SM treatment differ very little from those obtained by the 6D SM calculations, indicating that the frustrated translation mode is virtually decoupled from other vibrations present in our treatment.

Finally, we analyzed in some detail the level structure and assignment of excited in-plane frustrated translation mode which, as the lowest-frequency external vibration of CO/Cu(100), is the most important for understanding the surface dynamics.[10] Majority of the excited states inspected were assigned in terms of the quantum numbers of the 2D isotropic oscillator.

Work is in progress in our group on extending the quantum 6D treatment of adsorbate vibrations developed in this article to include the coupling with substrate phonons.

ACKNOWLEDGMENTS

This research has been supported in part by the National Science Foundation, through Grant CHE-9613641. We are grateful to Professor Joel M. Bowman (Emory University) for sending us the CO/Cu(100) potential, and also for providing the unpublished results of his 9D VSCF+CI calculations of CO/Cu(100).

[1] S. P. Lewis and A. M. Rappe, Phys. Rev. Lett. **77**, 5241 (1996).
[2] S. P. Lewis and A. M. Rappe, J. Chem. Phys. **110**, 4619 (1999).
[3] T. A. Germer, J. C. Stephenson, E. J. Heilwell, and R. R. Cavanagh, Phys. Rev. Lett. **71**, 3327 (1993).
[4] T. A. Germer, J. C. Stephenson, E. J. Heilwell, and R. R. Cavanagh, J. Chem. Phys. **101**, 1704 (1994).
[5] S. C. Park, J. M. Bowman, and D. A. Jelski, J. Chem. Phys. **104**, 2457 (1996).
[6] S. Carter, S. J. Culik, and J. M. Bowman, J. Chem. Phys. **107**, 10458 (1997).
[7] J. M. Bowman, Acc. Chem. Res. **19**, 202 (1986).
[8] R. B. Gerber and M. A. Ratner, Adv. Chem. Phys. **70**, 97 (1988).
[9] A. C. Luntz and J. Harris, Surf. Sci. **258**, 397 (1991).
[10] F. Hofmann and J. P. Toennies, Chem. Rev. **96**, 1307 (1996).
[11] A. P. Graham, F. Hofmann, J. P. Toennies, G. P. Williams, C. J. Hirschmugi, and J. Ellis, J. Chem. Phys. **108**, 7825 (1998).
[12] C. J. Hirschmugl, G. P. Williams, F. M. Hoffman, and Y. J. Chabal, Phys. Rev. Lett. **65**, 480 (1990).
[13] J. C. Tully, M. Gomez, and M. Head-Gordon, J. Vac. Sci. Technol. A **11**, 1914 (1993).
[14] J. T. Kindt, J. C. Tully, M. Head-Gordon, and M. A. Gomez, J. Chem. Phys. **109**, 3629 (1998).
[15] B. N. J. Persson and R. Ryberg, Phys. Rev. B **32**, 3586 (1985).
[16] S. Liu, Z. Bačić, J. W. Moskowitz, and K. E. Schmidt, J. Chem. Phys. **101**, 6359 (1994).
[17] S. Liu, Z. Bačić, J. W. Moskowitz, and K. E. Schmidt, J. Chem. Phys. **101**, 10181 (1994).
[18] S. Liu, Z. Bačić, J. W. Moskowitz, and K. E. Schmidt, J. Chem. Phys. **103**, 1829 (1995).

[19] J. Dai and J. C. Light, J. Chem. Phys. **107**, 1676 (1997).
[20] J. Dai and J. C. Light, J. Chem. Phys. **108**, 7816 (1998).
[21] G. J. Kroes, E. J. Baerends, and R. C. Mowrey, J. Chem. Phys. **107**, 3309 (1997).
[22] P. Saalfrank and W. H. Miller, Surf. Sci. **303**, 206 (1994).
[23] M. Mandziuk and Z. Bačić, J. Chem. Phys. **98**, 7165 (1993).
[24] Z. Bačić and J. C. Light, Annu. Rev. Phys. Chem. **40**, 469 (1989).
[25] Z. Bačić and J. C. Light, J. Chem. Phys. **85**, 4594 (1986).
[26] Z. Bačić and J. C. Light, J. Chem. Phys. **86**, 3065 (1987).
[27] A. Bach, S. Leutwyler, D. Sabo, and Z. Bačić, J. Chem. Phys. **107**, 8781 (1997).
[28] D. Sabo, Z. Bačić, S. Graf, and S. Leutwyler, J. Chem. Phys. **109**, 5404 (1998).
[29] J. Echave and D. C. Clary, Chem. Phys. Lett. **190**, 225 (1992).
[30] Q. Wu, D. H. Zhang, and J. Z. H. Zhang, J. Chem. Phys. **103**, 2548 (1995).
[31] Y. Qiu, J. Z. H. Zhang, and Z. Bačić, J. Chem. Phys. **108**, 4804 (1998).
[32] Z. Bačić and Y. Qiu, in *Advances in Molecular Vibrations and Collision Dynamics*, edited by Z. Bačić and J. M. Bowman (JAI, Greenwich, CT, 1998), Vol. III, p. 183.
[33] Z. Bačić, J. Chem. Soc., Faraday Trans. **93**, 1459 (1997).
[34] J. Dai and J. Z. H. Zhang, J. Chem. Phys. **102**, 6280 (1995).
[35] D. T. Colbert and W. H. Miller, J. Chem. Phys. **96**, 1982 (1992).
[36] J. M. Bowman (private communication).
[37] M. Bertino, J. Ellis, F. Hofmann, J. P. Toennies, and J. R. Manson, Phys. Rev. Lett. **73**, 605 (1994).
[38] J. Ellis, J. P. Toennies, and G. Witte, J. Chem. Phys. **102**, 5059 (1995).
[39] A. P. Graham, F. Hofmann, and J. P. Toennies, J. Chem. Phys. **104**, 5311 (1996).
[40] L. D. Landau and E. M. Lifshitz, *Quantum Mechanics* (Pergamon, Oxford, 1977).
[41] T. Droz, S. Leutwyler, M. Mandziuk, and Z. Bačić, J. Chem. Phys. **101**, 6412 (1994).
[42] E. B. Wilson, J. C. Decius, and P. C. Cross, *Molecular Vibrations: The Theory of Infrared and Raman Vibrational Spectra* (McGraw-Hill, New York, 1955).